Genomic Alterations of the *JAK2* and *PDL* Loci Occur in a Broad Spectrum of Lymphoid Malignancies

Katrien Van Roosbroeck[1,2], Julio Finalet Ferreiro[1], Thomas Tousseyn[3], Jo-Anne van der Krogt[1], Lucienne Michaux[1], Barbara Pienkowska-Grela[4], Ivan Theate[5], Pascale De Paepe[6], Daan Dierickx[7], Chantal Doyen[8], Natalie Put[1], Jan Cools[1,2], Peter Vandenberghe[1] and Iwona Wlodarska[1*]

[1]Center for Human Genetics, K.U.Leuven, Leuven, Belgium; [2]Center for the Biology of Disease, VIB, Leuven, Belgium; [3]Translational Cell and Tissue Research K.U.Leuven, Department of Pathology UZ Leuven, Leuven, Belgium; [4]Cytogenetic Laboratory, Maria Sklodowska-Curie Memorial Cancer Centre and Institute, Warsaw, Poland; [5]Service d'anatomopathologie, Cliniques universitaires Saint-Luc, Université catholique de Louvain, Brussels, Belgium; [6]Department of Pathology, AZ St Jan AV, Brugge, Belgium; [7]Department of Hematology, UZ Leuven, Leuven, Belgium and [8]Department of Hematology,Mont-Godinne University Hospital, Yvoir, Belgium.

* Correspondence to: Iwona Wlodarska, Center for Human Genetics, Herestraat 49, B-3000 Leuven, Belgium; e-mail: iwona.wlodarska@uzleuven.be; Phone: +32 16 34 60 57; Fax: +32 16 34 56 95

Short title: *JAK2* and *PDL1/2* aberrations in lymphoma

Supported by the concerted action grant from the K.U.Leuven no. 3M040406 (KVR, TT, JC, PV and IW) (http://www.kuleuven.be/), research grants from the FWO Vlaanderen (G081411N to TT) and “Stichting tegen Kanker” (PV) (http://www.kanker.be/). TT holds a Mandate for Fundamental and Translational Research from the “Stichting tegen Kanker” (2014-083). DD holds a Mandate for Clinical Research from the University Hospitals Leuven and is a fund manager of ‘Stefanie’s Rozen Fonds’. PV is a senior clinical investigator of the FWO-Vlaanderen.

Abstract

The recurrent 9p24.1 aberrations in lymphoid malignancies potentially involving four cancer-related and druggable genes (*JAK2*, *CD274/PDL1*, *PDCD1LG2/PDL2* and *KDM4C/JMJD2Cl*) are incompletely characterized. To gain more insight into the anatomy of these abnormalities, at first we studied 9p24.1 alterations in 18 leukemia/lymphoma cases using cytogenetic and molecular techniques. The aberrations comprised structural (nine cases) and numerical (nine cases) alterations. The former lesions were heterogeneous but shared a common breakpoint region of 200 kb downstream of *JAK2*. The rearrangements predominantly targeted the *PDL* locus. We have identified five potential partner genes of *PDL1/2*: *PHACTR4*/1p34, *N4BP2*/4p14, *EEF1A1*/6q13, *JAK2*/9p24.1 and *IGL*/22q11. Interestingly, the cryptic *JAK2-PDL1* rearrangement was generated by a microdeletion spanning the 3'*JAK2*-5'*PDL1* region. *JAK2* was additionally involved in a cytogenetically cryptic *IGH*-mediated t(9;14)(p24.1;q32) found in two patients. This rare but likely underestimated rearrangement highlights the essential role of *JAK2* in B-cell neoplasms. Cases with amplification of 9p24.1 were diagnosed as primary mediastinal B-cell lymphoma (five cases) and T-cell lymphoma (four cases). The smallest amplified 9p24.1 region was restricted to the *JAK2-PDL1/2-RANBP6* interval. In the next step, we screened 200 cases of classical Hodgkin lymphoma by interphase FISH and identified *PDL1/2* rearrangement (*CIITA*- and *IGH*-negative) in four cases (2%), what is a novel finding. Forty (25%) cases revealed high level amplification of 9p24.1, including four cases with a selective amplification of *PDL1/2*. Altogether, the majority of 9p24.1 rearrangements occurring in lymphoid malignancies seem to target the programmed death-1 ligands, what potentiates the therapeutic activity of PD-1 blockade in these tumors.

Keywords: *JAK2*, *PDL*, 9p24 translocation, amplification, lymphoma progression

INTRODUCTION

Genomic alterations of the 9p24.1 region, recurrent in hematological malignancies, have drawn a longstanding attention. The involved interval contains four cancer-related genes, *JAK2, CD274/PDL1, PDCD1LG2/PDL2* and *KDM4C/JMJD2CI*, all druggable targets for precision therapy (Sharma et al., 2011; Hao et al., 2014; Chin & Han, 2015). In addition to the 9p24.1 amplification hallmarking primary mediastinal B-cell lymphoma (PMBCL) and classic Hodgkin lymphoma (cHL) (Joos et al., 2000; Bentz et al., 2001; Meier et al., 2009; Green et al., 2010), all four genes are targeted by various leukemia/lymphoma-related rearrangements. The best known targeted gene, *JAK2,* encodes a non-receptor tyrosine kinase which plays a key role in the JAK-STAT signaling pathway downstream of several cytokine receptors (Ghoreschi et al., 2009). *JAK2* is frequently activated by mutations and chromosomal translocations in myeloproliferative disorders (Vainchenker et al., 2008; Skoda et al., 2015) and involved in recurrent rearrangements, including *SEC31A-JAK2* in cHL (Van Roosbroeck et al., 2011). *CD274 and PDCD1LG2* (further referred to as *PDL1* and *PDL2*, respectively) are coding for the programmed death-1 (PD-1) ligands, which act as negative regulators of anti-tumor immunity by binding their cognate receptor, PD-1, on cytotoxic T-cells, and which induce T-cell “exhaustion” (Blank & Mackensen, 2007; Keir et al., 2008; Zou & Chen, 2008; Andorsky et al., 2011). Rearrangements of the *PDL* loci were recently detected in 20% of PMBCL and in sporadic cases of primary testicular diffuse large B-cell lymphoma (DLBCL), primary central nervous system lymphoma and two HL-derived cell lines (Steidl et al., 2011; Twa et al., 2014; Berghoff et al., 2014; Twa et al., 2015). Thus far, three genes, *CIITA, IGH* and *NRG1*, were identified as *PDL*-fusion partners by high-throughput sequencing (Steidl et al., 2011; Twa et al., 2014; Twa et al., 2015; Twa & Steidl, 2015). *KDM4C* encodes a lysine-specific demethylase, which regulates histone methylation dynamics and plays critical roles in modulating chromatin architecture, gene transcription, and cellular differentiation (Berry & Janknecht, 2013). *KDM4C* is involved in a rare *IGH*-mediated translocation in mucosa-associated lymphoid tissue (MALT) lymphoma (Vinatzer et al., 2008). Noteworthy, the 9p24.1 amplification frequently observed in PMBCL and cHL, does not target a single gene, but affects at least 10 protein-coding genes, among others *JAK2, PDL1, PDL2* and *KDM4C*, located within the ~3.5 Mb commonly amplified interval (Rui et al., 2010). Following the concept of cooperative oncogenic effects of multiple genes within amplicons, the authors provided

evidence that *JAK2* and *KDM4C* cooperatively modify the epigenome of the amp(9p24.1)-positive lymphomas and, consequently, enhance proliferation and survival of neoplastic cells (Rui et al., 2010). On the other hand, an integrative genomic and transcriptomic study of Green et al., (Green et al., 2010) identified *PDL1* and *PDL2* as key targets of the 9p24.1 amplification in PMBCL and cHL, and showed that *JAK2* can additionally upregulate the expression of the *PDL* transcripts. The essential role of PDL1/2 in the pathogenesis of lymphoma is highlighted by an aberrant expression of these highly immunosuppressive proteins in other lymphoma subtypes, including certain aggressive B-cell lymphomas and virus-/immunodeficiency-associated malignancies (Chen et al., 2013; Berghoff et al., 2014). By expressing the PD-1 ligands, lymphomas, as well as other tumors, can selectively block antitumor immune responses (Andorsky et al., 2011). These findings have recently revolutionized the treatment of several solid tumors and hematologic malignancies (reviewed by Armand, 2015). Therapeutic blockade of PD-1 appeared to be particularly remarkable in cHL (Ansell et al., 2015), prompting further search of lymphomas that display similar features and might benefit of this novel form of therapy.

Most of the 9p24.1 discoveries in lymphoma come from interphase FISH studies, copy number analysis and high-throughput sequencing. Therefore, relatively little is known about chromosomal alterations underlying these rearrangements. To complete this knowledge and gain more insight into the anatomy of the 9p24.1 aberrations, we screened more than 40 leukemia/lymphoma cases with documented 9pter abnormalities and approximately 200 cases of unselected cHL by fluorescence *in situ* hybridization (FISH). Here, we report results of detailed molecular cytogenetic investigations of 26 cases of B- and T-cell malignancies, including cHL, with the cytogenetically and/or FISH-proven 9p24.1 alterations. The study demonstrates genetic heterogeneity and complexity of the 9p24.1 alterations in leukemia/lymphoma, which seem to predominantly target the *PDL* locus.

MATERIALS AND METHODS

Case Selection

Cases were identified through the Cancer Database of the Center for Human Genetics and Department of Pathology, UZ/KU Leuven, Leuven, Belgium. One case (no 1.2) was provided by Dr. Pienkowska-Grela

from MSCM Cancer Centre and Institute, Warsaw, Poland. Clinical information was retrieved for all cases from the medical records.

The study was reviewed and approved by the Ethical Committee of the KU Leuven, Leuven, Belgium. All samples were collected according to the institutional policies.

Cytogenetics

Conventional G-banding chromosomal analysis and FISH followed standard protocols. Karyotypes were described according to the International System for Human Cytogenetic Nomenclature (ISCN 2013) (Shaffer et al., 2013). FISH probes used in this study, as well as their genomic localization, can be found in **Table S1** and **Table S2**. Of note, the red-labelled probes included in the *JAK2* break-apart (BA) assay cover *PDL1* and *PDL2* genes located downstream of *JAK2* (**Figure 1A**). Noncommercial probes were directly labeled with SpectrumOrange- and SpectrumGreen-dUTP (Abbot Molecular, Ottigne, Belgium) using random prime reaction (Invitrogen, Carlsbad, USA). FISH experiments were evaluated using an Axioplan 2 fluorescence microscope equipped with a charge-coupled device Axiophot 2 camera (Carl Zeiss Microscopy, Jena, Germany) and a MetaSystems Isis imaging system (MetaSystems, Altlussheim, Germany). One to 10 abnormal metaphases (and facultatively 200 interphase cells) were evaluated in each FISH experiment. Interphase FISH analysis of cHL cases was previously described (Vandenberghe et al., 2015).

RNA Extraction and Quantitative Reverse Transcription PCR

Total RNA was extracted with TRIzol Reagent (Life Technologies, Merelbeke, Belgium), purified with the RNeasy Mini Kit (Qiagen, Dorking, United Kingdom) and treated with the Turbo DNA-*free*™ kit (Ambion, Austin, TX, USA) according to the manufacturer's instructions. One microgram of the DNase-treated total RNA was reverse transcribed into cDNA with random hexamers and SuperScript III (Life Technologies, Merelbeke, Belgium).

Quantitative reverse transcription (QRT)-PCR followed previously described protocols (Lahortiga et al., 2007), but was carried out on a cDNA template. Primer sequences used in QRT-PCR experiments can be found in **Table S3**. All QRT-PCR experiments were carried out in triplicate and normalized against the

HPRT1 reference gene. The fold difference was calculated with the ΔΔCq method and the expression of a mixture of five nonmalignant lymph node samples was set at one. Statistical analysis was done in GraphPad with the two-tailed unpaired t-test with a 95% confidence interval. p-values < 0.05 were considered statistically significant.

Copy Number Analysis

Whole-genome high-resolution analysis of four cases (no. 1.1, 1.4, 1.5 and 1.7) was performed with the Human Genome CGH Microarray 244A kit (Agilent Technologies, Santa Clara, CA) as previously described (Van Roosbroeck et al., 2011), but with some minor modifications. The ADM-2 algorithm was chosen to report aberrations for all the samples with a minimum of four probes per aberrant segment. The minimum absolute average log ratio was set at 0.22. Two cases (cases 1.6 and 1.9) were analyzed with the 2.7 M cytogenetic array from Affymetrix (Santa Clara, CA). The arrays were processed in accordance with the manufacturer's instructions. Raw data were analyzed with the Affymetrix software Chromosome Analysis Suite 1.1.0 (ChAS). For annotation information, the Cytogenetic Array Annotation files (Release 31) provided by Affymetrix, were used. For analysis of copy number alterations, a size of more than 100 kb and more than 20 markers/copy number alteration were used as thresholds.

RNA Sequencing

RNA sequencing was performed on the Illumina HiSeq2000 Genome Analyzer using a paired-end format. The RNA library preparation was carried out with the TRUseq RNA Sample Preparation Kit (Illumina, San Diego, CA) according to the manufacturer's instructions. Gene fusions were analyzed with the deFuse algorithm (McPherson et al., 2011) and ArrayStudio software (www.omicsoft.com).

Immunohistochemistry

Immunohistochemistry was performed on paraffin-embedded tissue sections with antibodies against PDL1 and PDL2 (ProSci Incorporated, Poway, CA). Sections were stained according to the manufacturer's recommendations, and staining results were visualized with the EnVision system (Dako, Glostrup, Denmark). Negative, as well as positive controls were included. Images were captured with a

Leica DM LB microscope (Leica, Wetzlar, Germany), a Leica PL FLUOTAR objective lens (40x/0.70) and a Leica DC200 camera. Images were imported directly into PowerPoint (Microsoft, Redmond, WA) with the Leica DC200 camera software (version 2.51).

RESULTS

Genetic Analysis

Forty one B-cell leukemia/lymphoma cases with structural 9pter abnormalities were subjected to metaphase FISH analysis with a dual-color *JAK2* BA assay. An aberrant FISH pattern was identified in 16 cases, including seven cases with rearranged signals (Table 1) and nine cases with amplified signals (Table 2). In the remaining cases, 9p breakpoints occurred either distal (13 cases) or proximal (12 cases) to *JAK2/PDLs*. The cases with breakpoints centromeric to *JAK2*/*PDLs* were additionally analyzed with the *KDM4C* BA assay (Table S2) and all showed a normal FISH pattern.

Table 1 presents seven cases with 9p24.1 rearrangements and two additional cases with apparently normal chromosomes 9, but with cryptic aberrations coincidentally detected by routine FISH (cases 1.2 and 1.9). The cases represent various indolent and aggressive B-cell malignancies, among others CLL in Richter transformation (case 1.1) and transformed MALT lymphoma (case 1.8). All 9p24.1 aberrations were further characterized by FISH and, if available, by array comparative genomic hybridization (aCGH), molecular techniques and RNA-sequencing (case 1.9). The aberrations were heterogeneous and included five reciprocal translocations (cases 1.1, 1.2, 1.5, 1.6 and 1.8), two non-reciprocal translocations (case 1.3), two insertions (cases 1.4 and 1.7) and one inversion (case 1.9). Two translocations, t(4;9)(p14;p24.1) and t(9;14)(p24.1;q32), were found in two cases each (cases 1.6 and 1.8; and cases 1.2 and 1.3, respectively). To characterize the 9p24.1 breakpoints more in-depth, we applied a set of 31 DNA probes covering the 9p21-9pter (~22 Mb) region. The detailed results of metaphase FISH analysis are summarized in Table S1. As shown in Figure 1A, all 9p24.1 breakpoints clustered in the 200 kb region centromeric to *JAK2,* harboring *PDL1* and *PDL2*. Intriguingly, in both cases with insertions (cases 1.4 and 1.7), cryptic microdeletions spanning *JAK2* and the neighboring sequences, but not affecting *PDL1/2*, were detected. In case 1.7, the deletion covered approximately 2 Mb region (9:3267306-5325065 bp), as estimated by aCGH profiling and confirmed by FISH (Figure S1). The centromeric breakpoint of this

deletion occurred approximately 104 kb telomeric to *PDL1* and was flanked by *RLN1* (retained) and *RLN2* (lost).

To identify partner genes involved in the 9p24.1 aberrations, all cases were analyzed by metaphase FISH with probes selected from the postulated reciprocal region (Table S1). The analysis demonstrated involvement of immunoglobulin (*IG*) genes (*IGL*/22q11 and *IGH*/14q32) in cases 1.1-1.3 (Figure 1B) and disruption of non-*IG* sequences in the remaining cases. In cases 1.4 and 1.5, the breakpoints were mapped in regions harboring the *PHACTR4* (1p34) and *EEF1A1* (6q13) genes, respectively. In cases 1.7, 1.6 and 1.8, the affected genes were not identified, but the breakpoints were narrowed down to the 3p21.3p24.3 cytoband (3:23600747-45463193 bp) and two overlapping 4p14 regions, 4:39927069-40657405 bp (*N4BP2, RHOH, CHRNA9, RBM47*) and 4:39781081-40087915 bp (*PDS5A, N4BP2*), respectively. Notably, both 4p14 breakpoints involved *N4BP2,* which might be a common target of this translocation. Interestingly, case 1.3 had likely unbalanced three-way t(9;13;14)(p24.1;q11;q32) associated with loss of der(13)t(13;14)(q11;q32)/*5'IGH* (green signal). Due to the 9p24.1 break between *C9orf46* and *PDL1*, the 9pter region harboring *JAK2* was translocated to the rearranged *IGH* locus at der(14), while *PDL1/2* were juxtaposed with the gene poor region at 13q11 (centromeric to RP11-341D18) on der(9). Very intriguing was case 1.9 with biallelic inv(9)(p23p24.1). As shown by aCGH (Figure 2A and 2C), the inversion was associated with two microdeletions: (i) at 9p24.1, spanning the 3' end of *JAK2* and the 5' region of *PDL1* (9:5048723-5458818 bp) and leading to the cryptic *JAK2-PDL1* rearrangement, and (ii) at 9p23, likely bordering the centromeric breakpoint of inv(9). As evidenced by SNP analysis and confirmed by FISH, the 9p aberrations were biallelic due to uniparental disomy of 9p (UPD9p) (Figure 2A-B). Subsequent RNA-sequencing identified the fusion of exon 4 of *JAK2* with genomic sequences 161 bp upstream of the *PDL1* transcript. These findings were validated by RT-PCR (**Figure 2D**). Due to the presence of a premature stop codon, the fusion protein was most likely not functional. As insulator sequences located directly upstream of *PDL1* were also deleted, the transcription machinery could use the *JAK2* promoter to aberrantly drive *PDL1* mRNA expression.

FISH analysis was complemented by aCGH performed in six cases (no. 1.1, 1.4, 1.5-1.7, and 1.9). We used aCGH data (partially shown) to verify and correct karyotypic abnormalities. Among others, aCGH detected cryptic del(9p21) involving *CDKN2A/B* in cases 1.6, 1.7 (**Figure S1**) and 1.9, and demonstrated

del(6q23)/*TNFAIP3* in cases 1.1, 1.5 and 1.6. The latter aberration was present in two additional cases not analyzed by aCGH.

Table 2 presents nine cases with amplified *JAK2* BA signals. The patients were diagnosed with PMBCL (no 2.1-2.5), PTCL NOS (no 2.6-2.7), ALK-negative ALCL (no. 2.8) and ALK-positive ALCL (no 2.9). Eight cases presented with add(9p), which was further specified as a homogeneously staining region (hsr). Case 2.4 displayed amplification outside of add(9p). The affected chromosomes showed heterogeneous morphology, underlied by a different size and structure of amplicons. For example, the long der(9p) in case 2.1 was generated by the 9pter-9pter fusion of two aberrant chromosomes 9 harboring hsr(9p24.1) varying in size. It seems that the initial amplicon underwent 'mirror' duplication, as deduced from the presence of two flanking signals of *CDKN2A*/9p21 (Figure 1C). The highest level of amplification was observed in cases 2.2 and 2.6 (Figure 1C). In case 2.3, the amplified *JAK2* BA signals were found on der(9) and subclonally, on derivatives of 14, 18 and 22. Three cases (2.2, 2.3 and 2.6) revealed hsr(9p) associated with non-reciprocal t(9p24), evidenced by a negative WCP 9 painting of the terminal region and loss of the 9p subtelomeric sequences. Because of a low percentage of neoplastic cells in the available material, the size of amplicons was not determined by aCGH but provisionally estimated by FISH with probes for the 9p-subtelomeric region, *KDM4C* (6.7 Mb), *NFIB* (14.08 Mb), *CDKN2A/B* (21.98 Mb) and *PAX5* (36.83 Mb) (Table S1 and Table S2). The smallest amplified region restricted to sequences spanned by the *JAK2* BA assay (*JAK2*<->*RANBP6*) was found in case 2.2 (Table 2).

Table 3 presents 8 selected cases of cHL with *PDL1/2* alterations detected by FISH in interphase Reed-Sternberg cells. The majority of these cases were identified during our previous FISH study of cHL (Van Roosbroeck et al., 2011). To date, we have analyzed approximately 200 cases of cHL and in four cases (no. 3.1-3.4) we have observed loss of the green/*JAK2* signal and retain of the red/*PDLs* signal indicative of an unbalanced t(9p24.1). Loss of 9pter was confirmed by FISH with the 9p subtelomeric probe. Lack of cytogenetic data prevented identification of partner genes, but involvement of *CIITA* and *IGH* in these translocations was excluded by FISH. It is worth to note, that the majority of analyzed cHL cases displayed copy number gain of the *JAK2* BA probes: 78 cases (39%) showed 3-5 extra signals (low copy gain) and 40 cases (25%) revealed amplified signals. Remarkably, four of the latter cases (no. 3.5-3.8) showed a predominant amplification of the red/*PDLs* signal (Figure 1D).

Expression Analysis

The expression pattern of five genes potentially targeted by the 9p24.1 aberrations detected in the first cohort, *JAK2*, *RLN1*, *C9orf46*, *PDL1* and *PDL2,* was assessed by QRT-PCR in seven available cases. The analysis demonstrated upregulation of *PDL1* and *PDL2* in case 1.4, overexpression of only *PDL1* in cases 1.7, 1.8 and 1.9, and upregulation of only *PDL2* in cases 1.1 and 1.5 (Table 1; Figure 3). No candidate gene was overexpressed in case 6. Further mRNA expression analysis of *JAK2*, *PDL1* and *PDL2* mRNA was performed in three PMBCL cases (no. 2.1, 2.2, 2.4) and single cases of PTCL NOS (no. 2.6) and ALK+ ALCL (no.2.9). The analysis detected overexpression of all three genes in cases 2.1 and 2.4 (the highest expression of *PDL1*), upregulation of *PDL1* and *PDL2* in case 2.2, upregulation of *JAK2* and *PDL1* in case 2.6 and overexpression of only *PDL1* in case 2.9 (Table 2). Results of QRT-PCR analysis performed in two T-cell lymphoma cases with amp(9p24.1) (cases 2.6 and 2.9) are shown in Figure 4.

Finally, available cases were studied by IHC with antisera for PDL1 and PDL2. All cases expressed at least one of the proteins analyzed (Table S4, Figure S2). Given, however, that lymphomas frequently express PD-1 ligands, the rearrangement-related overexpression of these proteins could not be demonstrated.

DISCUSSION

Our study provides evidence that the structural 9p24.1 aberrations in lymphoid malignancies are hallmarked by a common ~200 kb breakpoint region located downstream of *JAK2* and harboring *PDL1/2*. These rearrangements seem to target both loci and result in their transcriptional deregulation. As partner breakpoints affect (directly or indirectly) various protein-coding genes as well as protein-noncoding sequences, a fraction of the 9p24.1 rearrangements may escape detection by high-throughput sequencing. Involvement of *IG* loci, which was documented in t(9;14)(p24.1;q32) and t(9;22)(p24.1;q11), is typical for B-cell malignancies. The former translocation was found in two cases diagnosed as primary cutaneous DLBCL, leg-type, and B-ALL. Thus far, t(9;14)(p24.1;q32) has not been associated with these disease entities, but considering its cryptic nature, the translocation could be overlooked. Basing on the

known molecular mechanisms of t(*IG*) (Willis & Dyer, 2000; Kuppers & Dalla-Favera, 2001), we presume that t(9;14)(p24.1;q32) affects *JAK2*, because this gene, but not *PDL1/2*, was translocated to der(14) and juxtaposed with the 3'*IGH* enhancer. If so, *IGH-JAK2* would be the next *JAK2* rearrangement identified in B-ALL (Kawamura et al., 2015). This novel JAK2 aberration contrasts with the known *JAK2* fusions occurring in myeloid neoplasms and acute leukemias, like *ETV6-JAK2*, *BCR-JAK2*, *PCM1-JAK2* and others, which affect the 3'end of the gene and activate the JAK2 tyrosine kinase (Springuel et al., 2015). We presume that molecular consequences of t(9;14)(p24.1;q32) are similar to that of amp(9p24.1) and inactivated mutations of *SOCS1* (inhibitor of *JAK2*) recurrently occurring in PMBCL (Melzner et al., 2005). The latter aberrations lead to elevated transcription of the entire *JAK2*, followed by phosphorylation of the product and subsequent activation of the JAK2/STAT pathway and its targets (e.g. *CCND1, OSM, BCLxL*). Given that *JAK2* can additionally upregulate expression of the *PDL* transcripts (Green et al., 2010), t(9;14)(p24.1;q32) may also indirectly affect the expression of PD-1 ligands.

Noteworthy, all the remaining 9p24.1 aberrations, including the *IGL*-mediated t(9;22)(p24.1;q11), target the *PDL* locus. In contrast to t(9;14)(p24.1;q32), the variant t(9;22)(p24.1;q11) translocates strong regulatory sequences of *IGL* to der(9) and upregulates expression of *PDL2*, as shown by QRT-PCR. Intriguingly, the translocation was detected at the time of Richter transformation of a trisomy 12-positive CLL, suggesting its essential role in disease progression. This finding places the *PDL2* gene together with *MYC*, *BCL3*, *BMI1* and *NOTCH1* on a list of genes implicated in high grade transformation of CLL (Martin-Subero et al., 2007; De Keersmaecker et al., 2012; Put et al., 2012; Rouhigharabaei et al., 2013).

Mechanisms of deregulation of the *PDL* locus by non-*IG* partner sequences have not been completely deciphered. In some cases, transcription of *PDL1/2* was probably driven by promoters of partner genes, i.e., *PHACTR4*/1p34, *N4BP2*/4p14, *EEF1A1*/6q13 and *JAK2*/9p24.1, like in the previously reported fusions (Steidl et al., 2011; Twa et al., 2014; Twa et al., 2015; Twa & Steidl, 2015). Noteworthy, the cryptic *JAK2-PDL1* rearrangement was generated by a microdeletion spanning the 3'*JAK2*-5'*PDL1* region. The effect of this fusion was enhanced by a subsequent UPD9p resulting in duplication of the whole 9p. On the other hand, upregulation of the *PDL* locus by der(9)t(9;13)(p24.1;q13) involving the gene poor region at 13q11, might be caused by a position effect and/or loss of negative regulatory sequences at 9p24.1. The latter mechanism(s) could be also implicated in both insertions,

ins(3;9)(p?24.3;p24.1p?13) and ins(9;1)(p24.1;p34p36), showing deletion of sequences telomeric to the 9p24.1 breakpoint. Mechanistic significance of the 9pter/*JAK2* loss is supported by a recurrent occurrence of similar lesions in cHL. Basing on FISH data, we presume that the 9p24.1 rearrangements in cHL represent unbalanced translocations targeting the *PDL* locus and associated with loss of 9pter/*JAK2*. Potential partner genes, if any, comprise neither *CIITA*, known to be involved in the *PDL1/2* fusions in PMBCL (Steidl et al., 2011), nor *IGH*, engaged in the *PDL2-IGV7-81* fusion in one cHL-derived cell line (Twa et al., 2014). Further studies of the *PDL1/2* rearrangements in cHL are needed to elucidate molecular mechanisms underlying these lesions.

As mentioned above, the most frequent 9p24.1 aberration in lymphoma, particularly in PMBCL and cHL, is amplification of the terminal interval spanning *JAK2, PDL1, PDL2* and *KDM4C*. Notably, the aberration is detectable in circulating cell free DNA from cHL cases (Vandenberghe et al., 2015) and may serve as biomarker in non-invasive diagnostic/follow up testing. Also in the present series of selected tumors with 9pter abnormalities, approximately half of cases (56%) showed amplification of the *JAK2/PDLs* signals. These cases were diagnosed either as PMBCL, or T-cell lymphoma (PTCL NOS, ALK-/ALK+ ALCL). Strikingly, none of the PMBCL cases with 9p aberrations revealed *PDL1/2* rearrangement, although these aberrations seem to mark 20% of PMBCL (Steidl et al., 2011). Of note, we narrowed down the smallest amplified 9p24.1 region to the *JAK2-PDL1/2-RANBP6* interval, miminizing the role of *KDM4C* in amp(9p24.1)-positive lymphomas (Rui et al., 2010). The amp(9p24.1) was detected in 25% of unselected cHL analyzed by interphase FISH, which is in line with previous reports (Joos et al., 2000; Meier et al., 2009; Green et al., 2010). Although the majory of cHL cases displayed a balanced *JAK2/PDLs* amplification, selective amplification of the *PDL* locus was observed in several cases. Interestingly, we have described a similar amplification peak affecting *PDL1/2* in a recently analyzed case of EBV+ posttransplant DLBCL, one of two EBV+ DLBCL subtypes showing recurrent amp(9p24.1) (Finalet Ferreiro et al., 2015). Altogether, we showed that 9p24.1 aberrations in B-cell malignancies directly or indirectly affect the genes coding ligands for PD-1. Previous studies showed that the PDL/PD-1 pathway plays an important role in immune evasion of tumor cells. The immunosuppresive ligands expressed on tumor cells interact with the co-inhibitory PD-1 on T cells mediating decreased TCR-mediated proliferation and cytokine production (Blank & Mackensen, 2007). Functional *in vitro* and *in vivo* studies performed on

lymphoma cell lines and mouse models demonstarted that PDL1 knockdown inhibits tumor proliferation, decreases tumor invasion ability and inhibits cell cycle progression. In addition, downregulation of PDL1 reverses drug-resistance and increase apoptosis of tumor cell (Li et al., 2012). Based on emerging association between the PDL/PD-1 pathway, T-cell exhaustion and tumor progression, novel immunotherapies targeting PD-1 has been recently developed. Several clinical trials of the PD-1 blockade have already been successfully conducted in hematological malignancies and particularly high response rate was obtained in patients with cHL (reviewed by Armand, 2015).

Summaring, our study confirms the previously published findings of recurrent structural and copy number alterations of 9p24.1 in lymphoid malignancies. The rearrangements are cytogenetically and molecularly heterogeneous but share the same 'hot' breakpoint region downstream of *JAK2*. They predominantly affect the *PDL* locus and lead to an aberrant expression of PD-1 ligands favoring an immune evasion (Blank & Mackensen, 2007; Green et al., 2010). The *PDL1/2* rearrangements are not specific but feature a broad spectrum of lymphoid malignancies, among others CLL, and contribute in their progression and increased aggressiveness. Amplification of 9p24.1, frequent in PMBCL and cHL, was also detected in T-cell lymphomas, confirming the previously reported data (present report and Meier et al., 2009). Structural aberrations of *PDL1/2* and their selective amplification in cHL, which are novel findings, highlight an essential role of the *PDL* locus in the pathogenesis of cHL. As recently shown, the T-cell 'exhaustion" which resulted from an aberrant expression of PDL1/2 by neoplastic cells, is reversible with PD-1 blockade (Ansell et al., 2015). Systematic screening of entities which emerged in our study is warranted to identify individuals who may benefit in future from the anti-PD-1 therapy.

SUPPLEMENTAL INFORMATION

The Supplemental Information includes four tables and two figures, and can be found online with this article.

ACKNOWLEDGMENTS

The authors would like to thank Ursula Pluys, Kathleen Doms and Emilie Bittoun for their excellent technical assistance and Rita Logist for the editorial help.

REFERENCES

Andorsky DJ, Yamada RE, Said J, Pinkus GS, Betting DJ, Timmerman JM. 2011. Programmed death ligand 1 is expressed by non-hodgkin lymphomas and inhibits the activity of tumor-associated T cells. Clin Cancer Res 17:4232-4244.

Ansell SM, Lesokhin AM, Borrello I, Halwani A, Scott EC, Gutierrez M, Schuster SJ, Millenson MM, Cattry D, Freeman GJ, Rodig SJ, Chapuy B, Ligon AH, Zhu L, Grosso JF, Kim SY, Timmerman JM, Shipp MA, Armand P. 2015. PD-1 blockade with nivolumab in relapsed or refractory Hodgkin's lymphoma. N Engl J Med 372:311-319.

Armand P. 2015. Checkpoint blockade in lymphoma. Blood 125:393-400.

Bentz M, Barth TF, Bruderlein S, Bock D, Schwerer MJ, Baudis M, Joos S, Viardot A, Feller AC, Muller-Hermelink HK, Lichter P, Dohner H, Moller P. 2001. Gain of chromosome arm 9p is characteristic of primary mediastinal B-cell lymphoma (MBL): comprehensive molecular cytogenetic analysis and presentation of a novel MBL cell line. Genes Chromosomes Cancer 30:393-401.

Berghoff AS, Ricken G, Widhalm G, Rajky O, Hainfellner JA, Birner P, Raderer M, Preusser M. 2014. PD1 (CD279) and PD-L1 (CD274, B7H1) expression in primary central nervous system lymphomas (PCNSL). Clin Neuropathol 33:42-49.

Berry WL, Janknecht R. 2013. KDM4/JMJD2 histone demethylases: epigenetic regulators in cancer cells. Cancer Res 73:2936-2942.

Blank C, Mackensen A. 2007. Contribution of the PD-L1/PD-1 pathway to T-cell exhaustion: an update on implications for chronic infections and tumor evasion. Cancer Immunol Immunother 56:739-745.

Chen BJ, Chapuy B, Ouyang J, Sun HH, Roemer MG, Xu ML, Yu H, Fletcher CD, Freeman GJ, Shipp MA, Rodig SJ. 2013. PD-L1 expression is characteristic of a subset of aggressive B-cell lymphomas and virus-associated malignancies. Clin Cancer Res 19:3462-3473.

Chin YW, Han SY. 2015. KDM4 histone demethylase inhibitors for anti-cancer agents: a patent review. Expert Opin Ther Pat 25:135-144.

De Keersmaecker K, Michaux L, Bosly A, Graux C, Ferreiro JF, Vandenberghe P, Cools J, Wlodarska I. 2012. Rearrangement of NOTCH1 or BCL3 can independently trigger progression of CLL. Blood 119:3864-3866.

Finalet Ferreiro J, Morscio J, Dierickx D, Marcelis L, Vandenberghe P, Gheysens O, Verhoef G, Zamani M, Tousseyn T, Wlodarska I. 2015. EBV-Positive and EBV-Negative Posttransplant Diffuse Large B-Cell Lymphomas have Distinct Genomic and Transcriptomic Features. Am J Transplant in press.

Ghoreschi K, Laurence A, O'Shea JJ. 2009. Janus kinases in immune cell signaling. Immunol Rev 228:273-287.

Green MR, Monti S, Rodig SJ, Juszczynski P, Currie T, O'Donnell E, Chapuy B, Takeyama K, Neuberg D, Golub TR, Kutok JL, Shipp MA. 2010. Integrative analysis reveals selective 9p24.1 amplification, increased PD-1 ligand expression, and further induction via JAK2 in nodular sclerosing Hodgkin lymphoma and primary mediastinal large B-cell lymphoma. Blood 116:3268-3277.

Hao Y, Chapuy B, Monti S, Sun HH, Rodig SJ, Shipp MA. 2014. Selective JAK2 inhibition specifically decreases Hodgkin lymphoma and mediastinal large B-cell lymphoma growth in vitro and in vivo. Clin Cancer Res 20:2674-2683.

Joos S, Kupper M, Ohl S, von BF, Mechtersheimer G, Bentz M, Marynen P, Moller P, Pfreundschuh M, Trumper L, Lichter P. 2000. Genomic imbalances including amplification of the tyrosine kinase gene JAK2 in CD30+ Hodgkin cells. Cancer Res 60:549-552.

Kawamura M, Taki T, Kaku H, Ohki K, Hayashi Y. 2015. Identification of SPAG9 as a novel JAK2 fusion partner gene in pediatric acute lymphoblastic leukemia with t(9;17)(p24;q21). Genes Chromosomes Cancer 54:401-408.

Keir ME, Butte MJ, Freeman GJ, Sharpe AH. 2008. PD-1 and its ligands in tolerance and immunity. Annu Rev Immunol 26:677-704.

Kuppers R, Dalla-Favera R. 2001. Mechanisms of chromosomal translocations in B cell lymphomas. Oncogene 20:5580-5594.

Lahortiga I, De Keersmaecker K, Van Vlierberghe P, Graux C, Cauwelier B, Lambert F, Mentens N, Beverloo HB, Pieters R, Speleman F, Odero MD, Bauters M, Froyen G, Marynen P, Vandenberghe P, Wlodarska I, Meijerink JP, Cools J. 2007. Duplication of the MYB oncogene in T cell acute lymphoblastic leukemia. Nat Genet 39:593-595.

Li Y, Wang J, Li C, Ke XY. 2012. Contribution of PD-L1 to oncogenesis of lymphoma and its RNAi-based targeting therapy. Leuk Lymphoma 53:2015-2023.

Martin-Subero JI, Ibbotson R, Klapper W, Michaux L, Callet-Bauchu E, Berger F, Calasanz MJ, De Wolf-Peeters C, Dyer MJ, Felman P, Gardiner A, Gascoyne RD, Gesk S, Harder L, Horsman DE, Kneba M, Kuppers R, Majid A, Parry-Jones N, Ritgen M, Salido M, Sole F, Thiel G, Wacker HH, Oscier D, Wlodarska I, Siebert R. 2007. A comprehensive genetic and histopathologic analysis identifies two subgroups of B-cell malignancies carrying a t(14;19)(q32;q13) or variant BCL3-translocation. Leukemia 21:1532-1544.

McPherson A, Hormozdiari F, Zayed A, Giuliany R, Ha G, Sun MG, Griffith M, Heravi MA, Senz J, Melnyk N, Pacheco M, Marra MA, Hirst M, Nielsen TO, Sahinalp SC, Huntsman D, Shah SP. 2011. deFuse: an algorithm for gene fusion discovery in tumor RNA-Seq data. PLoS Comput Biol 7:e1001138.

Meier C, Hoeller S, Bourgau C, Hirschmann P, Schwaller J, Went P, Pileri SA, Reiter A, Dirnhofer S, Tzankov A. 2009. Recurrent numerical aberrations of JAK2 and deregulation of the JAK2-STAT cascade in lymphomas. Mod Pathol 22:476-487.

Melzner I, Bucur AJ, Bruderlein S, Dorsch K, Hasel C, Barth TF, Leithauser F, Moller P. 2005. Biallelic mutation of SOCS-1 impairs JAK2 degradation and sustains phospho-JAK2 action in the MedB-1 mediastinal lymphoma line. Blood 105:2535-2542.

Put N, Van Roosbroeck K, Konings P, Meeus P, Brusselmans C, Rack K, Gervais C, Nguyen-Khac F, Chapiro E, Radford-Weiss I, Struski S, Dastugue N, Gachard N, Lefebvre C, Barin C, Eclache V, Fert-Ferrer S, Laibe S, Mozziconacci MJ, Quilichini B, Poirel HA, Wlodarska I, Hagemeijer A, Moreau Y, Vandenberghe P, Michaux L. 2012. Chronic lymphocytic leukemia and prolymphocytic leukemia with MYC translocations: a subgroup with an aggressive disease course. Ann Hematol 91:863-873.

Rouhigharabaei L, Ferreiro JF, Put N, Michaux L, Tousseyn T, Lefebvre C, Gardiner A, De Kelver W, Demuynck H, Verschuere J, Theate I, Vicente C, Vandenberghe P, Cools J, Wlodarska I. 2013. BMI1, the polycomb-group gene, is recurrently targeted by genomic rearrangements in progressive B-cell leukemia/lymphoma. Genes Chromosomes Cancer 52:928-944.

Rui L, Emre NC, Kruhlak MJ, Chung HJ, Steidl C, Slack G, Wright GW, Lenz G, Ngo VN, Shaffer AL, Xu W, Zhao H, Yang Y, Lamy L, Davis RE, Xiao W, Powell J, Maloney D, Thomas CJ, Moller P, Rosenwald A, Ott G, Muller-Hermelink HK, Savage K, Connors JM, Rimsza LM, Campo E, Jaffe ES,

Delabie J, Smeland EB, Weisenburger DD, Chan WC, Gascoyne RD, Levens D, Staudt LM. 2010. Cooperative epigenetic modulation by cancer amplicon genes. Cancer Cell 18:590-605.

Shaffer LG, McGowfan-Jordan J, Schmid M. 2013. An International System for Human Cytogenetic Nomenclature (2013). Basel, Switzerland: S. Karger AG.

Sharma P, Wagner K, Wolchok JD, Allison JP. 2011. Novel cancer immunotherapy agents with survival benefit: recent successes and next steps. Nat Rev Cancer 11:805-812.

Skoda RC, Duek A, Grisouard J. 2015. Pathogenesis of myeloproliferative neoplasms. Exp Hematol 43:599-608.

Springuel L, Renauld JC, Knoops L. 2015. JAK kinase targeting in hematologic malignancies: a sinuous pathway from identification of genetic alterations towards clinical indications. Haematologica 100:1240-1253.

Steidl C, Shah SP, Woolcock BW, Rui L, Kawahara M, Farinha P, Johnson NA, Zhao Y, Telenius A, Neriah SB, McPherson A, Meissner B, Okoye UC, Diepstra A, van den Berg A, Sun M, Leung G, Jones SJ, Connors JM, Huntsman DG, Savage KJ, Rimsza LM, Horsman DE, Staudt LM, Steidl U, Marra MA, Gascoyne RD. 2011. MHC class II transactivator CIITA is a recurrent gene fusion partner in lymphoid cancers. Nature 471:377-381.

Twa DD, Chan FC, Ben-Neriah S, Woolcock BW, Mottok A, Tan KL, Slack GW, Gunawardana J, Lim RS, McPherson AW, Kridel R, Telenius A, Scott DW, Savage KJ, Shah SP, Gascoyne RD, Steidl C. 2014. Genomic rearrangements involving programmed death ligands are recurrent in primary mediastinal large B-cell lymphoma. Blood 123:2062-2065.

Twa DD, Mottok A, Chan FC, Ben-Neriah S, Woolcock BW, Tan KL, Mungall AJ, McDonald H, Zhao Y, Lim RS, Nelson BH, Milne K, Shah SP, Morin RD, Marra MA, Scott DW, Gascoyne RD, Steidl C. 2015. Recurrent genomic rearrangements in primary testicular lymphoma. J Pathol 236:136-141.

Twa DD, Steidl C. 2015. Structural genomic alterations in primary mediastinal large B-cell lymphoma. Leuk Lymphoma e-pub ahead of print:1-12.

Vainchenker W, Dusa A, Constantinescu SN. 2008. JAKs in pathology: role of Janus kinases in hematopoietic malignancies and immunodeficiencies. Semin Cell Dev Biol 19:385-393.

Van Roosbroeck K, Cox L, Tousseyn T, Lahortiga I, Gielen O, Cauwelier B, De PP, Verhoef G, Marynen P, Vandenberghe P, De Wolf-Peeters C, Cools J, Wlodarska I. 2011. JAK2 rearrangements, including the novel SEC31A-JAK2 fusion, are recurrent in classical Hodgkin lymphoma. Blood 117:4056-4064.

Vandenberghe P, Wlodarska I, Tousseyn T, Dehaspe L, Dierickx D, Verheecke M, Uyttebroeck A, Bechter O, Delforge M, Vandecaveye V, Brison N, Verhoef G, Legius E, Amant F, Vermeesch J. 2015. Non-invasive detection of genomic imbalances in Hodgkin/Reed-Sternberg cells in early and advanced stage Hodgkin's lymphoma by sequencing of circulating cell-free DNA: a technical proof-of-principle study. The Lancet Haematology 2:e55-e65.

Vinatzer U, Gollinger M, Mullauer L, Raderer M, Chott A, Streubel B. 2008. Mucosa-associated lymphoid tissue lymphoma: novel translocations including rearrangements of ODZ2, JMJD2C, and CNN3. Clin Cancer Res 14:6426-6431.

Willis TG, Dyer MJ. 2000. The role of immunoglobulin translocations in the pathogenesis of B-cell malignancies. Blood 96:808-822.

Zou W, Chen L. 2008. Inhibitory B7-family molecules in the tumour microenvironment. Nat Rev Immunol 8:467-477.

LEGEND TO THE FIGURES

Figure 1. Physical map of the 9p24.1 breakpoint cluster and FISH examples of structural and numerical 9p24.1 aberrations in lymphoma. (A) Physical map of the 9p24.1 breakpoint cluster of approximately 200 kb downstream of *JAK2* defined in cases 1.1-1.9. Yellow boxes represent genes, blue boxes represent probes, and red and green boxes represent the probes from the *JAK2* BA assay. (B) FISH analysis of case 1.1 with t(9;22)(p24.1;q11) using the *JAK2* BA assay (left panel) and WI2-1621G6-SO/ WI2-1844L21-SG (middle panel), and case 1.2 with t(9;14)(p24.1;q32) using LSI IGH (right panel) and *JAK2* BA probes (inset). (C) Metaphase FISH analysis with probes covering *JAK2* (red) and *CDKN2A* (green), and WCP9/SpectrumGreen (inset) in cases 2.1 (left panel), 2.2 (middle panel) and 2.6 with amp(9p24). (D) Interphase FISH analysis with the *JAK2* BA assay and CEP8/SA (blue) probes in two cHL cases with structural 9p24 aberrations (case 3.2, left panel; case 3.4, middle panel) and amp(9p24) (case 3.7, right panel).

Figure 2. Complex 9p aberrations in case 1.9 with inv(9). (A) Upper panel: aCGH profile of the whole chromosome 9 showing three microdeletions at 9p24.1 (*JAK2-PDL1*), 9p23 and 9p21 (*CDKN2A/B*) pointed by red arrows. Lower panel: SNP data illustrating UPD9p. Due to the low percentage of neoplastic cells (20%) in the analyzed specimen, 9p microdeletions were recognized by the software as monoallelic, however, FISH demonstrated biallelic 9p losses and rearrangements (see B). (B) Interphase FISH analysis with the *JAK2* BA probes (left panel), RP11-125K10-SG/RP11-509D8-SO (middle panel) and RP11-140C18-SO/RP11-343D17-SG (right panel) evidencing biallelic 9p24.1 rearrangements/deletions. (C) aCGH profile of 9p24.1 showing a microdeletion spanning 3'*JAK2* and 5'*PDL1*/*CD274* (marked in green). (D) Schematic representation of the genomic structure of the *JAK2/PDL1* region and the *JAK2-PDL1* rearrangement determined by RNA-sequencing (upper panel) and validated by RT-PCR (lower panel). Breakpoint regions are indicated by black arrows.

Figure 3. Expression analysis of *JAK2, PDL1* and *PDL2* mRNA in cases with structural 9p24.1 abnormalities. (A) *JAK2* is significantly downregulated in 6/7 analyzed cases (marked with **) as compared to the average expression in five nonmalignant lymph nodes; (B) *PDL1* is significantly upregulated in 4/7

analyzed cases (marked with *) as compared to the average expression in five nonmalignant lymph nodes; (C) *PDL2* is significantly upregulated in 3/7 analyzed cases (marked with *) and significantly downregulated in 3/7 cases (marked with **) as compared to the average expression in five non-malignant lymph nodes.

Figure 4. QRT-PCR analysis of *JAK2*, *PDL1* and *PDL2* performed in two T-NHL patients with 9p24.1 amplification. (A) Both *JAK2* and *PDL1* are significantly upregulated in a case 2.6 (PTCL NOS), as compared to the average expression in five non-malignant lymph nodes. (B) Only *PDL1* is significantly upregulated in a case 2.9 (ALK+ ALCL), as compared to the average expression in five non-malignant lymph nodes. *JAK2* and *PDL2* are significantly downregulated in this patient.

Tables

Table 1: Relevant genetic and clinical data of cases with structural 9p24.1 aberrations

Case n°	Sex/Age	Diagnosis	Treatment	Response/ Survival	Sample/ Status	Cytogenetics[a]	FISH mapped breakpoints		QRT-PCR				
							9p24.1	Partner chromosome	*JAK2*	*RLN1*	*C9orf46*	*PDL1*	*PDL2*
1.1[b]	M/70	CLL in RT	CHOPx6; cerebral RDT; palliative care	PR/died 14 months after diagnosis	LN/P	47,XY,del(5)(p13.3p15.1),del(6)(q15),t(9;22)(p24.1;q11),+12,der(22)t(1;22)(q11;q13)[3]	Between WI2-1621G6 and WI2-1844L21	*IGL*/22q11 (*IGL* BA and CTD-2507C12 split)	down	down	down	NL	13.3-fold up
1.2	M/69	Primary cutaneous DLBCL, leg-type	R-CHOPx8, RDT	PR	TM/D	ND .ish t(9;14)(p24.1;q32)	Between WI2-1844L21 and WI2-2110N11	*IGH*/14q32 (LSI IGH split)	ND	ND	ND	ND	ND
			IVACx2	PR/died 15 months after diagnosis	TM/P	43~49,XY,t(1;9)(q21;q34)[5],add(2)(p2?3)[13],+3[11],+add(3)(p13)[3],der(5)t(5;10)(q22;q21),del(6)(q23)[3], del(8)(p21)[15],t(9;14)(p24.1;q32),-10,+add(12)(p13)[6],add(15)(q26)[5],del(17)(p11.2), +18[13],+2-3mar][cp18]	Between WI2-1844L21 and WI2-2110N11	*IGH*/14q32 (LSI IGH split)	ND	ND	ND	ND	ND
1.3	M/75	B-ALL	ND	ND	BM/D	47,XY,der(2)t(2;9)(q13;q31),del(6)(q22),del(8)(p21), der(9)t(9;13)(p24.1;q11)t(2;9)(q13;q31),+add(9)(q13), -13, der(14)t(9;14)(p24.1;q32),-19,+3mar[5]	Between WI2-1621G6 and WI2-1844L21	*IGH*/14q32 (LSI IGH split; RP11-417P24 and 11771 separated) Unknown/13q11 (centromeric to RP11-341D18)	ND	ND	ND	ND	ND
1.4[b]	M/62	MALT lymphoma	Splenectomy, R-CHOP x8	PD, died 77 months after diagnosis (DR)	S/D	46-47,XY,del(1)(p34p36),t(4;6)(q35;q13),ins(9;1)(p24.1;p34p36),+i(9)(p10)[7],der(13)t(X;13)(p11;p11), add(14)(q32),add(19)(q13)[cp11]	Between WI2-1621G6 and WI2-1844L21	*PHACTR4*/1p34 (RP11-427O24 and RP4-669K10 separated)	NL	down	NL	11.4-fold up	3.3-fold up
1.5[b]	M/18	DLBCL	R-CHOP like**	CR/alive 120 months after diagnosis	LN/P	48,XY,+X,der(4)t(2;4)(p12;p15.1)[9],t(5;16)(q33;p13), t(6;9)(q13;p24),del(6)(q21q23),+8[19]	Within WI2-592M24	Unknown (*EEF1A1*<-> *MTO1)*/6q13 (RP11-705N21 and RP11-772H06 separated)	down	ND	ND	NL	5.6-fold up
1.6[c]	M/61	B-LL	PROMACE-MOPP; palliative care at relapse	CR/relapse/died 84 months after diagnosis (within 1 month after relapse)	BM/P	47-48,X,+r(X),Y,del(2)(q12q21),t(4;9)(p14;p24),i(6)(p10), del(8)(q11q13),del(9)(p21p21),+der(9)t(4;9)(p14;p24)[3], dup(12)(q12q21)[3],i(18)(q10)[3],add(19)(q13)[4][cp11]	Between WI2-2110N11 and WI2-2834C19	?*N4BP2*/4p14 (RP11-306G03 and RP11-666I40 separated)	down	down	down	NL	down

1.7[b]	M/61	MZL	R-CHOPx6, FCRx4 + Ritux x2; Watch and wait	died 90 months after diagnosis from secondary AML (in 2d CR of NHL)	LN/D	49,XY,+X,**ins(3;9)(p?24.3;p24.1p?13)**,t(5;9)(q13;p21), del(6)(q13q16.3),+7,del(9)(p13p24.2), +18[18]	Between WI2-424I14 and WI2-1790I11	Unknown/3p21.3p24.3 (RP11-89F18 and RP11-111P21 separated)	down	down	NL	1.5-fold up	NL
1.8	F/69	DLBCL (transformed MALT lymphoma)	Reduction of immune-suppression, Rx4	PD/died within 3 months (DR)	LN/P	46,XX,del(3)(q21)[4],**t(4;9)(p14;p24)**,add(10)(q11)[6],t(14;18)(q32;q12)[12]	Between WI2-1621G6 and WI2-1844L21	?*N4BP2*/4p14 *(*RP11-391N20 and RP11-306G03 separated)	down	ND	ND	6.6-fold up	down
1.9[c]	M/49	FL, grade II -IIIa	Watch and wait (7 months); R-CHOPx8 and Ritux x2	CR/alive 64 months after diagnosis	LN/D	46,XY,t(2;14)(p24;q32),**inv(9)(p23q24.1)**x2, del(9p21p21)x2,dup(12)(q13.11q21.1)[13]	Telomeric to WI2-2110N11	*JAK2*/9p24.1 *(JAK2 BA* split)	down	ND	ND	1.4-fold up	down

Abbreviations: M, male; F, female; CLL, chronic lymphocytic leukemia; RT, Richter transformation; DLBCL, diffuse large B-cell lymphoma; B-ALL, B-cell acute lymphoblastic leukemia; MALT, mucosa-associated lymphoid tissue; B-LL, B-cell lymphoblastic lymphoma; MZL, marginal zone lymphoma; FL, follicular lymphoma; (R)-CHOP, (rituximab)-cyclophosphamide, doxorubicin, vincristine, prednisone; RDT, radiotherapy; IVAC, ifosfamide, etoposide, high-dose cytarabine; ND, not determined; PROMACE-MOPP, prednisone, methotrexate, doxorubicin, cyclophosphamide, etoposide, mechlorethamine, vincristine, procarbazine; FCR, fludarabine, cyclophosphamide, rituximab; PR, partial remission; CR, complete remission; PD, progressive disease; LN, lymph node; P, progression; TM, tumor (skin); D, diagnosis; BM, bone marrow; S, spleen.

[a] Corrected after FISH and aCGH; 9p aberrations appear in bold characters

[b] Cases analyzed by aCGH (244k arrays of Agilent)

[c] Cases analyzed by SNP arrays (2.7 M arrays of Affymetrix)

Table 2: FISH and QRT-PCR analysis of lymphoma cases with 9p24.1 amplification

Case	Sex/Age	Diagnosis	Sample	Karyotype[a]	JAK2 BA pattern	Range of amplicon	QRT-PCR		
							JAK2	*PDL1*	*PDL2*
2.1	F/37	PMBCL	Med/D	46,XX,add(6)(q27),**der(9)(9qter->hsr9p24::hsr9p24->9qter)**,der(16)t(10;16)(q11;p13)[2],+mar[3]	2 amplicons on der(9)	9pter<->*NFIB*	4.9-fold up	17.3-fold up	14.7-fold up
2.2	M/35	PMBCL	Med/D	50-51,XY,der(7)t(7;7)(p22;q11)[8],**+der(9) add(9)(p24)hsr(9)(p24)**,add(14)(q32),+2-5 mar,inc[9]	high-level amplification on add(9p24) and 2 signals on mar1	*JAK2*<->*RANBP6*	NL	6.8-fold up	5.0-fold up
2.3	F/27	PMBCL	Med/D	48-50,XX,+X,del(3)(q25),add(3)(q27),der(7)del(7)(p15)ins(7;?)(q22;?),**+der(9)add(9)(p24)hsr(9)(p24),** add(14)(q32),add(18)(q22)[2],add(19)(p13),add(22)(q13)[2],+2mar[cp10]	triplicated signals on der(9), add(14), add(18) and add(22)	9pter<->*NFIB*	ND	ND	ND
2.4	F/31	PMBCL	Med/D	50,XX,+X,+5,add(9)(p21),add(14)(q32),del(18)(q21),+2mar[4]	amplicons on two markers	NA	7.2-fold up	30.6-fold up	10.4-fold up
2.5	F/46	PMBCL	Med/D	45-50,XX,add(2)(p24)[9],del(3)(q23)[8],del(6)(q23q25)[6],+7[9],**hsr(9)(p24)**,+12[7],add(14)(q32)[4],+del(18)(q21)[3],+20[7],+21[8],+mar1[6],+mar2[2][cp16]	1 amplicon on hsr(9p24)	*JAK2*<->*KMD4C*	ND	ND	ND
2.6	M/62	PTCL NOS/ CLL	S/D	46,XY,add(1)(p36)[8],del(4)(q31q34),del(6)(q13q23),**der(9)add(9p24)hsr(9)(p24)**,der(17)t(5;17)(q13;p11)[18].ish.del(13)(q14/*RB1*) (67%)	1 amplicon on der(9) (high-level amplification)	*JAK2*<->*KMD4C*	3.5-fold up	3.4-fold up	NL
2.7	M/38	PTCL NOS	BM/P	46,XY,add(5)(q35),**hsr(9)(p24)**,add(21)(p13)[6]	4 amplicons on hsr(9p)	*JAK2*<->*NFIB*	ND	ND	ND
2.8	M/40	ALK- ALCL	LN/P	Polyploid (4N),add(1)(p36),add(2)(p24),dup(4)(q?),del(5)(p12),del(6)(q23),dup(7)(p22p15),**hsr(9)(p24)**,dup(11)(q23q24),add(13)(q34),add(14)(q31),+>10mar,inc[13]	1 amplicon on hsr(9p24)	*JAK2*<->*KMD4C*	ND	ND	ND
2.9	M/9	ALK+ ALCL	LN/D	48,XY,+X,t(2;5)(p23;q35),**hsr(9)(p24)**,del(17)(p11),+19[10]	1 amplicon on hsr(9p24)	*JAK2*<->*KMD4C*	down	2.7-fold up	down

Abbreviations: F, female; M, male; PMBCL, primary mediastinal B-cell lymphoma; PTCL NOS, peripheral T-cell lymphoma, not otherwise specified; CLL, chronic lymphocytic leukemia; ALK, anaplastic lymphoma kinase; ALCL, anaplastic large cell lymphoma; Med, mediastinum; S, spleen; BM, bone marrow; LN, lymph node; D, diagnosis; P, progression; NL, normal; ND, not determined;

[a]9p aberrations appear in bold characters

Table 3. FISH analysis of selected Hodgkin lymphoma cases with 9p24.1 aberrations

Case	Diagnosis	FISH results	Conclusion
3.1	NSHL	*JAK2* BA/CEP 8 (SA): 3F4R/3B 5'*JAK2* (SG)/*PDL1-PDL2* (SO): 3F3R *CIITA* BA: 3-4F LSI *IGH*: 3-4F	unbalanced t(9p24.1) with bkpt between *JAK2* (lost) and *PDL1/2*
3.2	NSHL	*JAK2* BA/CEP8 (SA): 3F1R/2B 5'*JAK2* (SG)/*PDL1-PDL2* (SO): 3F1G *CIITA* BA: 3F *IGH* BA: 3F	unbalanced t(9p24.1) with bkpt between *JAK2* (lost) and *PDL1/2*
3.3	NSHL	*JAK2* BA: 5-7F2R 5'*JAK2* (SG)/*PDL1-PDL2* (SO): 3-7F1-2R *CIITA* BA: 3F *IGH* BA: 3F	unbalanced t(9p24.1) with bkpt between *JAK2* (lost) and *PDL1/2*
3.4	NSHL	*JAK2* BA/CEP8 (SA): 1F2R/3B RP11-509D8 (SG)/RP11-140C18 (SO): 1F *PDL1/PDL2*: 3F *CIITA* BA: 3F *IGH* BA: 3F	unbalanced t(9p24.1) with bkpt between *JAK2* (lost) and *PDL1/2*
3.5	NSHL	*JAK2* BA/CEP8 (SA): 5-8F/3B; 5-7F 1amp(Rpred)/3B	copy number gain of *JAK2* BAP and a suclonal amplification of *PDL1/2*
3.6	NSHL	*JAK2* BA:2-4F1amp(Rpred)	amplification of 9p24.1 with a predominant gain of *PDL1/2*
3.7	HL NOS	*JAK2* BA/CEP8 (SA): 2F2amp(Rpred)/3-4B;4-7F4-5amp(Rpred)/5-11B	amplification of 9p24.1 with a predominant gain of *PDL1/2*
3.8	MCHL	*JAK2* BA/CEP8 (SA):3-5F2GRamp/3B	amplification of *PDL1/2*

Abbreviations: NSHL, nodular sclerosis Hodgkin lymphoma; HL NOS, Hodgkin lymphoma, not otherwise specified; MCHL, mixed cellularity Hodgkin lymphoma; BA, break apart; SA, spectrum aqua (blue); SG, spectrum green (green); SO, spectrum orange (red); F, fused signal; R4, red signal; G, green signal; B, blue signal; amp, amplified signal; Rpred, predominant red signal; bkpt, breakpoint

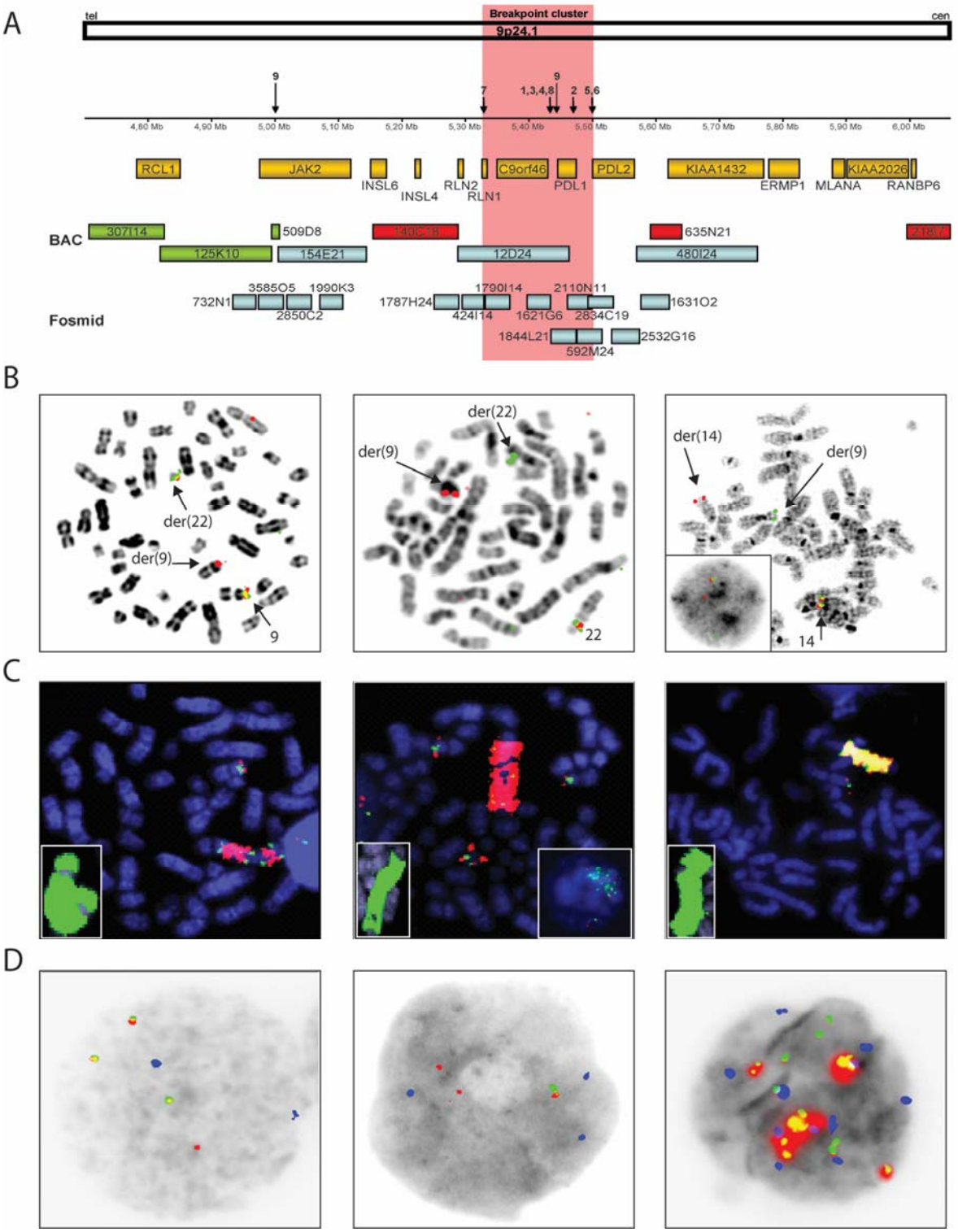
A
tel
Breakpoint cluster
9p24.1
cen
9
7
1,3,4,8
9
2
5,6
4,80 Mb
4,90 Mb
5,00 Mb
5,10 Mb
5,20 Mb
5,30 Mb
5,40 Mb
5,50 Mb
5,60 Mb
5,70 Mb
5,80 Mb
5,90 Mb
6,00 Mb
RCL1
JAK2
INSL6
INSL4
RLN2
RLN1
C9orf46
PDL1
PDL2
KIAA1432
ERMP1
KIAA2026
MLANA
RANBP6
BAC
307I14
509D8
635N21
125K10
154E21
12D24
480I24
Fosmid
3585O5
1990K3
732N1
2850C2
1790I14
2110N11
1787H24
424I14
1621G6
2834C19
1631O2
1844L21
2532G16
592M24
B
der(22)
der(9)
9
der(22)
der(9)
22
der(14)
der(9)
14
C
D

Figrue 1

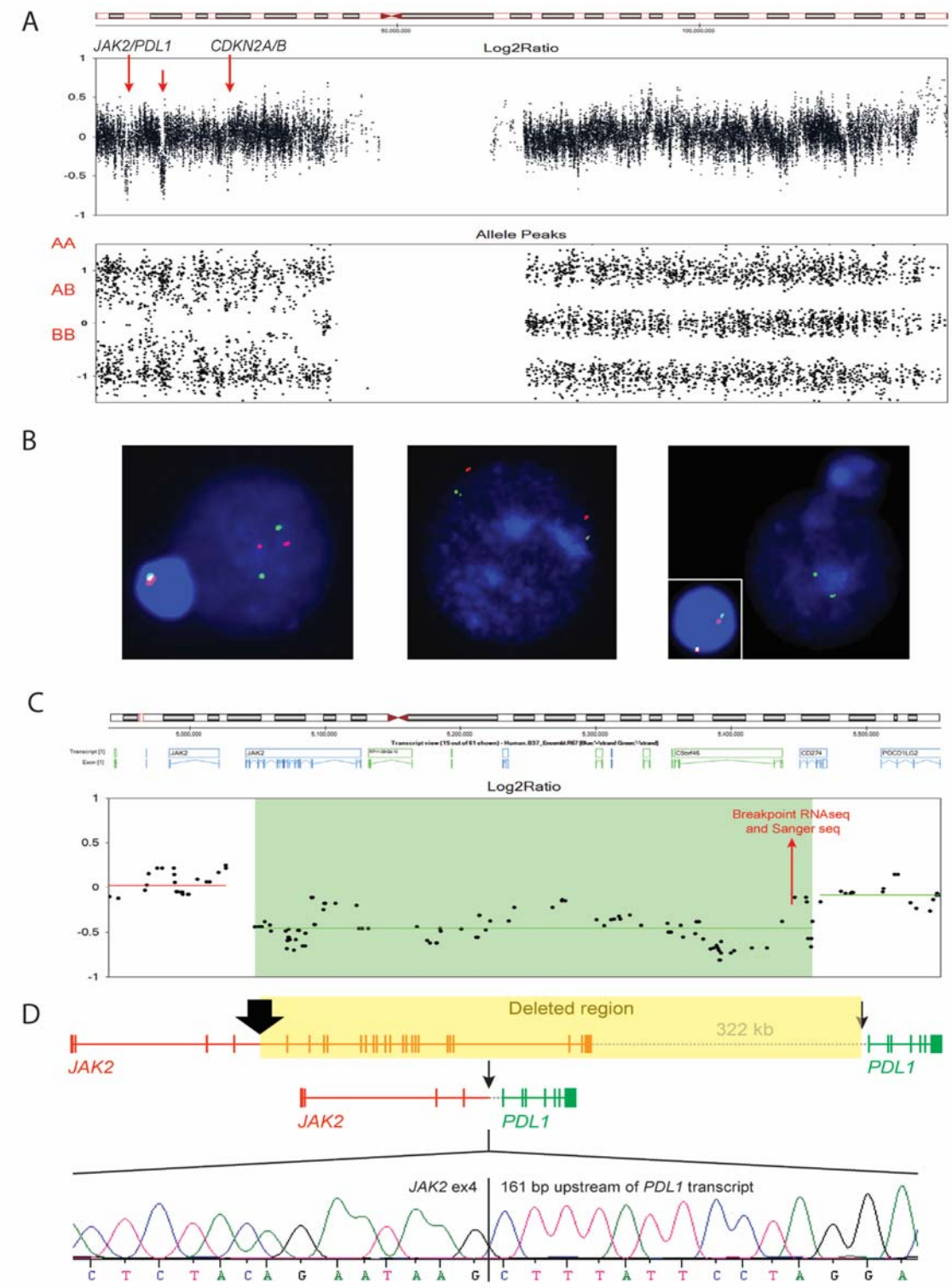
A
JAK2/PDL1
CDKN2A/B
Log2Ratio
Allele Peaks
AA
AB
BB
B
C
Log2Ratio
Breakpoint RNAseq
and Sanger seq
D
Deleted region
322 kb
JAK2
PDL1
JAK2
PDL1
JAK2 ex4
161 bp upstream of PDL1 transcript
C T C T A C A G A A T A A G C T T T A T T C C T A G G A

Figure 2

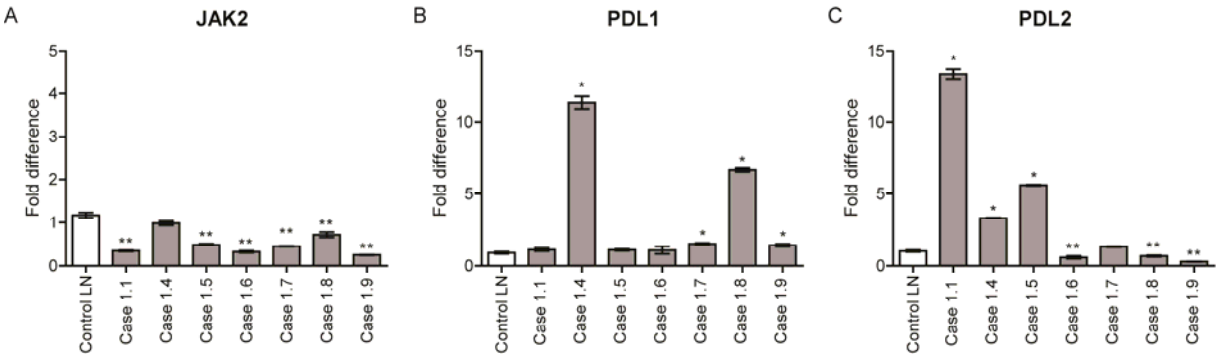
A
JAK2
Fold difference
Control LN
Case 1.1
Case 1.4
Case 1.5
Case 1.6
Case 1.7
Case 1.8
Case 1.9
B
PDL1
C
PDL2

Figure 3

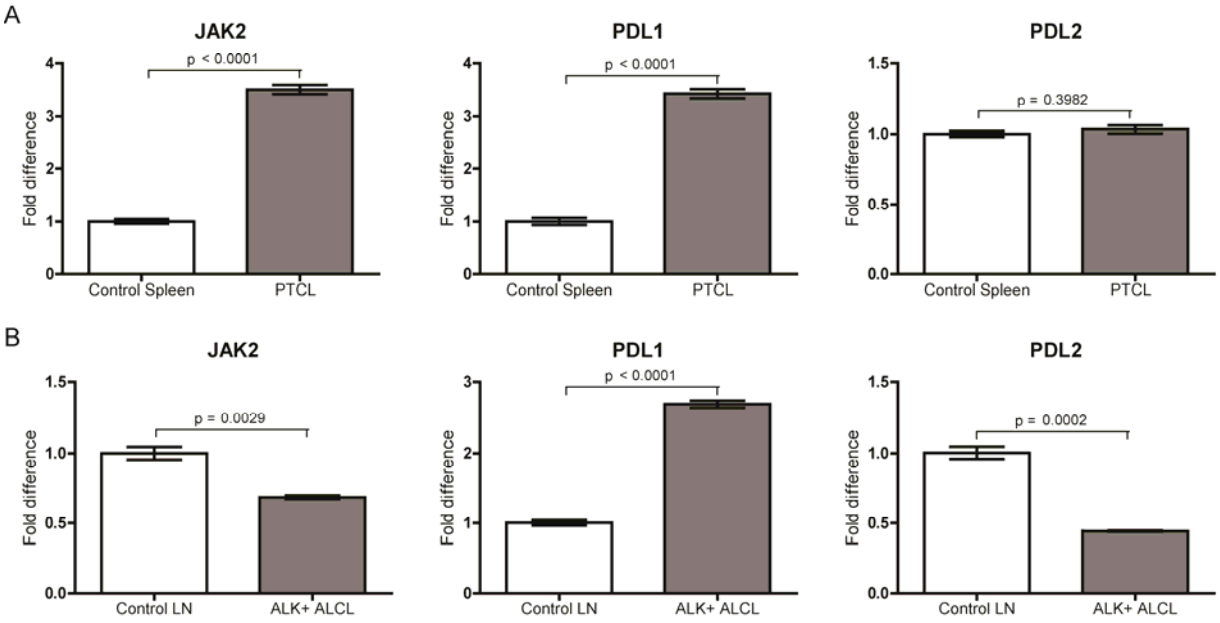
A
JAK2
p < 0.0001
Fold difference
Control Spleen
PTCL
PDL1
p < 0.0001
Fold difference
Control Spleen
PTCL
PDL2
p = 0.3982
Fold difference
Control Spleen
PTCL
B
JAK2
p = 0.0029
Fold difference
Control LN
ALK+ ALCL
PDL1
p < 0.0001
Fold difference
Control LN
ALK+ ALCL
PDL2
p = 0.0002
Fold difference
Control LN
ALK+ ALCL

Figure 4

Supporting Information

Four Supporting Tables:

Supplemental Table S1. FISH analyses of B-cell leukemia/lymphoma cases with structural 9p24 abnormalities.

Supplemental Table S2. Additional FISH probes

Supplemental Table S3: Primers used in QRT-PCR and RT-PCR experiments

Supplemental Table S4: Summary of IHC results

Two Supporting Figures:

Supporting Figure S1. The 9p24.1 alterations in patient 1.7. (A) Partial karyotype illustrating involvement of 9p in two aberrations: ins(3;9)(p?24.3;p24.1p13) (red arrows) and t(5;9)(q13;p21) (blue arrows). (B) Examples of FISH with the *JAK2* BA assay (left) and WI2-1621G6-SO/WI2-2110N11-SG covering *PDL1* (right). Note loss of the *JAK2*/green signal and presence of *PDL1* signals on ins(3;9) and der(5). (C) aCGH profile of chromosome 9 with two microdeletions detected at 9p21/*CDKN2A* and 9p24.1/*JAK2*. (D) The centromeric breakpoint of the 9p24.1 deletion located between *JAK2* and *PDL1/2* (marked in pink).

Supporting Figure S2. Examples of immunohistochemistry using antisera against PDL1 and PDL2 in different lymphoma types harboring structural and numerical 9p24.1 aberrations. (A-C) PDL1 is expressed in the diffuse neoplastic cells in cases with B-cell NHL, PMBCL and T-cell lymphoma. Due to the predominance of neoplastic cells, expression of PDL1 in the accompanying stromal cells cannot be evaluated. PDL2 is weakly expressed in the nucleus (and or cytoplasm) of lymphomas, but no obvious expression in the stromal cells. (D-E) In the Hodgkin/Reed-Sternberg cells (HRS, circled) PDL1 is strongly expressed in a combined membranous and cytoplasmic pattern. A weaker cytoplasmic PDL1 expression is seen in the cytoplasm of the majority of stromal cells. (T: tumor cells; S: stromal cells; N: necrosis). Note a strong expression of PDL2 in the cytoplasm (and potentially nucleus) of the HRS cells, and weaker, partial cytoplasmic expression in the accompanying stromal cells.

Supplemental References

1. Knight SJ, Lese CM, Precht KS, Kuc J, Ning Y, Lucas S, Regan R, Brenan M, Nicod A, Lawrie NM, Cardy DL, Nguyen H, Hudson TJ, Riethman HC, Ledbetter DH, Flint J. 2000. An optimized set of human telomere clones for studying telomere integrity and architecture. Am J Hum Genet 67:320-332.
2. Poulsen TS, Silahtaroglu AN, Gisselo CG, Gaarsdal E, Rasmussen T, Tommerup N, Johnsen HE. 2001. Detection of illegitimate rearrangement within the immunoglobulin locus on 14q32.3 in B-cell malignancies using end-sequenced probes. Genes Chromosomes Cancer 32:265-274.
3. Poulsen TS, Silahtaroglu AN, Gisselo CG, Tommerup N, Johnsen HE. 2002. Detection of illegitimate rearrangements within the immunoglobulin light chain loci in B cell malignancies using end sequenced probes. Leukemia 16:2148-2155.

Supporting Tables

Table S1. FISH analyses of B-cell leukemia/lymphoma cases with structural 9p24 abnormalities.

	Probes	Localization (Mb)	Case 1.1		Case 1.2		Case 1.3			Case 1.4		Case 1.5		Case 1.6		Case 1.7		Case 1.8		Case 1.9[a]	
			der(9)	der(22)	der(9)	der(14)	der(9)	der(14)	mar[b]	der(9)	der(1)	der(9)	der(6)	der(9)	der(4)	der(9)	der(3)	der(4)	der(9)	inv(9)	inv(9)
Chr 9	9p subtel	(1)	ND	ND	ND	ND	ND	ND	ND	+	-	ND	ND	ND	ND	+	-	ND	ND	ND	ND
	RP11-307I14	4,721,083-4,831,655	-	+	-	+	-	+	+	-	-	-	+	-	+	-	-	+	-	+	+
	RP11-125K10	4,831,656-5,001,841	-	+	-	+	-	+	+	-	-	-	+	-	+	-	-	+	-	+	+
	WI2-732N1	4,942,238-4,979,354	-	+	ND	ND	-	+	+	ND	ND	ND	ND	-	+	-	-	ND	ND	ND	ND
	WI2-3585O5	4,982,186-5,022,801	-	+	ND	ND	-	+	+	ND	ND	ND	ND	-	+	-	-	ND	ND	ND	ND
	RP11-509D8	5,001,842-5,018,809	-	+	-	+	-	+	+	-	-	-	+	-	+	-	-	+	-	dim/mv	dim/mv
	RP11-154E21	5,017,179-5,144,221	ND	ND	ND	ND	ND	ND	ND	ND	ND	ND	ND	ND	ND	ND	ND	ND	ND	-	-
	WI2-2850C2	5,026,385-5,066,923	-	+	ND	ND	-	+	+	ND	ND	ND	ND	-	+	-	-	ND	ND	ND	ND
	WI2-1990K3	5,078,327-5,116,150	-	+	ND	ND	-	+	+	ND	ND	ND	ND	-	+	-	-	ND	ND	ND	ND
	RP11-140C18	5,189,856-5,298,020	-	+	-	+	-	+	+	-	-	-	+	-	+	-	-	+	-	-	-
	WI2-1787H24	5,260,851-5,300,296	ND	ND	ND	ND	-	+	+	ND	ND	ND	ND	-	+	-	-	ND	ND	ND	ND
	WI2-424I14	5,303,176-5,337,602	ND	ND	ND	ND	-	+	+	ND	ND	ND	ND	-	+	-	-	ND	ND	ND	ND
	WI2-1790I14	5,339,442-5,379,592	ND	ND	ND	ND	-	+	+	ND	ND	ND	ND	-	+	-	+	ND	ND	ND	ND
	WI2-1621G6	5,408,033-5,445,949	-	+	-	+	-	+	+	-	-	-	+	-	+	-	+	+	-	ND	ND
	WI2-1844L21	5,445,912-5,485,647	+	-	-	+	+	-	+	+	-	ND	ND	-	+	ND	ND	-	+	ND	ND
	WI2-2110N11	5,470,306-5,509,331	+	-	+	-	+	-	+	+	-	-	+	-	+	-	+	-	+	+/mv	+/mv
	WI2-592M24	5,485,309-5,525,738	ND	ND	+	-	ND	ND	ND	+	-	+ (weak)	+	ND	ND	ND	ND	ND	ND	ND	ND
	WI2-2834C19	5,501,423-5,543,929	ND	ND	+	-	ND	ND	ND	ND	ND	+	-	+	-	-	+	-	+	+/mv	+/mv
	WI2-2532G16	5,539,271-5,582,268	ND	ND	ND	ND	ND	ND	ND	ND	ND	+	-	ND	ND	-	+	ND	ND	ND	ND
	RP11-480I24	5,571,006-5,760,432	ND	ND	+	-	ND	ND	ND	ND	ND	ND	ND	ND	ND	ND	ND	-	+	ND	ND
	WI2-1631O2	5,587,603-5,630,859	ND	ND	ND	ND	ND	ND	ND	+	-	+	-	+	-	-	+	ND	ND	ND	ND
	RP11-635N21	5,600,740-5,649,598	+	-	+	-	+	-	+	+	-	+	-	+	-	-	+	-	+	+/mv	+/mv
	RP11-717B10	5,789,062-5,937,516	ND	ND	+	-	ND	ND	ND	ND	ND	ND	ND	ND	ND	ND	ND	ND	ND	ND	ND
	RP11-218I7	6,005,678-6,072,142	+	-	+	-	+	-	+	ND	ND	ND	ND	ND	ND	-	+	-	+	ND	ND
	RP11-41J05	6,223,060-6,398,690	ND	ND	+	-	ND	ND	ND	ND	ND	ND	ND	ND	ND	ND	ND	ND	ND	ND	ND
	RP11-247G05	6,363,061-6,508,614	ND	ND	+	-	ND	ND	ND	ND	ND	ND	ND	ND	ND	ND	ND	ND	ND	ND	ND
	RP11-723E16	6,493,417-6,641,755	ND	ND	+	-	ND	ND	ND	ND	ND	ND	ND	ND	ND	ND	ND	ND	ND	ND	ND
	RP11-580K10	7,295,409-7,450,317	ND	ND	+	-	ND	ND	ND	ND	ND	ND	ND	ND	ND	ND	ND	ND	ND	ND	ND

	RP11-343D17	9,199,596-9,383,041	ND	ND	+	-	ND	ND	ND	+	-	ND	ND	ND	ND	-	+	ND	ND	+	+
	RP11-447H12	9,599,884-9,759,173	ND	ND	ND	ND	ND	ND	ND	+	-	ND	ND	ND	ND	-	+	ND	ND	ND	ND
	LSI CDKN2A	Vysis	-	-	ND	ND	-	-	-	+	-	+	-	-	-	-	ND	ND	ND	-	-
Chr 22	RP11 274M7	23,052,633-23,214,673	-	+																	
	CTD-2507C12	23,180,066-23,355,157	+	+																	
	RP11-165G5	23,250,860-23,406,965	+	-																	
Chr 14	LSI IGH BA	Vysis			G	R	-	R	-												
	RP11-417P24	106,196,305-106,364,512			ND	ND	-	+	-												
	BAC-11771	(2)			ND	ND	-	-	-												
Chr 13	RP11-341D18	18171249-18358106					+	-	-												
	LSI 13 (RB1)	Vysis					+	-	-												
	LSI D13S319	Vysis					+	-	-												
Chr 1	RP11-49J3	5,945,552-6,043,853								+	-										
	RP4-635E18	11,065,710-11,176,478								+	-										
	RP4-745E8	20,607,566-20,686,231								+	-										
	RP11-132G19	22,051,359-22,224,520								+	-										
	RP11-509F14	24,626,576-24,634,037								+	-										
	RP11-304H10	24,727,422-24,908,172								+	-										
	RP4-633N17	27,360,930-27,479,943								+	-										
	RP1-144C9	27,702,736-27,780,057								+	-										
	RP1-159A19	27,857,725-27,981,011								+	-										
	RP11-427O24	28,057,537-28,202,673								+	-										
	RP4-669K10	28,829,017-28,962,836								-	-										
	RP5-893G23	30,541,692-30,628,950								-	+ (weak)										
	RP5-1090M5	37,395,519-37,526,758								-	+										
	RP5-1034F7	43,575,745-43,650,761								-	+										
	RP11-184I16	44,150,334-44,249,955								-	+										
Chr 6	RP11-462G2	71,064,771-71,126,997										-	+								
	RP11-111D8	72,103,204-72,112,282										-	+								
	RP11-256L9	73,124,203-73,160,829										-	+								
	RP11-374I18	73,530,353-73,688,036										-	+								
	RP11-138M05	73,627,395-73,786,422										-	+								
	RP11-328E03	73,842,334-74,019,788										-	+								

	RP11-705N21	74,050,342-74,215,080					-	+						
	RP11-772H06	74,227,958-74,418,453					+	-						
	RP11-319B24	74,665,118-74,850,704					+	-						
	RP11-34L4	75,244,618-75,245,128					+	-						
Chr 4	4p subtel	(1)							+	-			-	+
	LSI IGH/FGFR3	Vysis							ND	ND			-	+
	RP11-278E22	36,161,294-36,318,582							ND	ND			-	+
	RP11-36B15	37,515,691-37,674,760							ND	ND			-	+
	RP11-433F02	39,631,305-39,779,414							+	-			-	+
	RP11-391N20	39,781,081-39,964,888							+	-			-	+
	RP11-306G03	39,927,069-40,087,915							+	-			+	-
	RP11-666I10	40,509,029-40,657,405							-	+			+	-
	RP11-52K10	40,667,673-40,816,069							ND	ND			+	-
	RP11-599P02	41,055,576-41,203,917							ND	ND			+	-
	RP11-764C19	44,347,824-44,533,551							ND	ND			+	-
Chr 3	GS-1186-B18	3psubtel (1)									-	+		
	RP11-89F18	23,431,548-23,600,747									-	+ /sep[d]		
	RP11-111P21	45,463,193-45,522,973									-	+ /sep[d]		

Abbreviations: +, present; -, absent; ND, not determined; dim, diminished; sep, separated; mv, moved

[a]We postulate a number of complex genetic events that occurred in this patient, including
(i) Three microdeletions at 9p24.1, 9p23 and 9p21/*CDKN2A/B*; the former spans the 3' end of *JAK2* and the region flanking the 5' end of *PDL1*.
(ii) Inversion of 9p likely associated with 9p23 and 9p24.1 microdeletions; the telomeric breakpoint of the 9p24.1 microdeletion probably occurred between 125K10 and 509D8 (Figure1A). The FISH mapping of the centromeric breakpoint of inv(9) is challanging due to a small region which was targeted by the inversion.
(iii) Uniparental disomy of 9p (9p UPD) covering 9p11.2p24.3, including the region affected by three microdeletions and the *JAK2-PDL1* rearrangement. FISH, SNP array and molecular findings in this case are illustrated in Figure 1C-E.
[b]Extra copy of *JAK2* BAP signal was found on a marker chromosome. Array CGH detected a duplication of the 9p24.3-9p24.1 region (1 Mb-7,487,100 Mb) harboring *JAK2*, *PDL1* and *PDL2*.
[c]Vysis LSI CDKN2A was applied to validate aCGH/SNP array findings of mono-/bi-allelic deletion of *CDKN2A* and *CDKN2B* detected in 5/7 analyzed cases.
[d]separation of RP11-89F18/-111P21 signals indicate that the 9p24.1 region was inserted at 3p21.31p24.3 centromeric to RP11-89F18 and telomeric to RP11-111P21.

Breakpoint region
Monoallelic deletion
Biallelic deletion
Duplication
Region of insertion

Table S2. Additional FISH probes

Cytoband/gene	Probes	Genomic localization (hg 19)	Reference
9p24.1 (*KMD4C*)	RP11-151G19 (SO)	6043367-6219086	www.ensembl.org
	RP11-346G4 (SO)	6270398-6466928	www.ensembl.org
	RP11-927L8 (SG)	7080501-7274185	www.ensembl.org
	RP11-958H5 (SG)	7291535-7471568	www.ensembl.org
9p23/22.3 (*NFIB*)	RP11-1107G7	14148116-14343128	www.ensembl.org
9p13.2 (*PAX5*)	RP11-243F8	36844939-37033208	www.ensembl.org

Table S3: Primers used in QRT-PCR and RT-PCR experiments

JAK2 ex22-F	5’-AGA ACC TGG TGA AAG TCC CAT ATT-3’
JAK2 ex23-R	5’-TGA GGC CAC AGA AAA CTT GCT-3’
RLN1 ex2-F	5’-CGA CCC TAC GTG GCA CTG T-3’
RLN1 ex2-R	5’-GCA ATA TTT AGC AAG AGA CCT TTT GG-3’
C9orf46 ex2-F	5’-GCG TCC TCT AAC ACA TTC AGA CTA CA-3’
C9orf46 ex2-3-R	5’-TAT AAA CCC CAT TTT GAC CTC TTT CT-3’
PDL1 ex5-F	5’-CCT TGG TGT AGC ACT GAC ATT CA-3’
PDL1 ex6-R	5’-TGG ATG CCA CAT TTT TTC ACA-3’
HPRT1 ex6-F	5’-TGA CAC TGG CAA AAC AAT GCA-3’
HPRT1 ex6-7-R	5’-GGT CCT TTT CAC CAG CAA GCT-3’
JAK2-PDL1 Pair 1-F	5'-GGT ATC CAC CCA ACC ATG TCT TCC A-3'
JAK2-PDL1 Pair 1-R	5'-TGC CGG GCG TTG GAC TTT CC-3'
JAK2-PDL1 Pair 2-F	5'-TCC ATC TGG GGA GTA TGT TGC AGA-3'
JAK2-PDL1 Pair 2-R	5'-GCC GGG CGT TGG ACT TTC CT-3'

Table S4: Summary of IHC results

Cases no.	Diagnosis	Nº of analyzed cases	Nº of cases positive for	
			PDL1[a]	PDL2[a]
1.1-1.9	various	6	4	5
2.1-2.5	PMBCL	5	5	5
2.6-2.9	T-NHL	3	3	2
3.1-3.5	cHL	5	4	3
3.6-3.8	cHL	3	3	3

[a]Expression of at least one PDL protein was detected in almost all cases analyzed

A


3
5
9

B

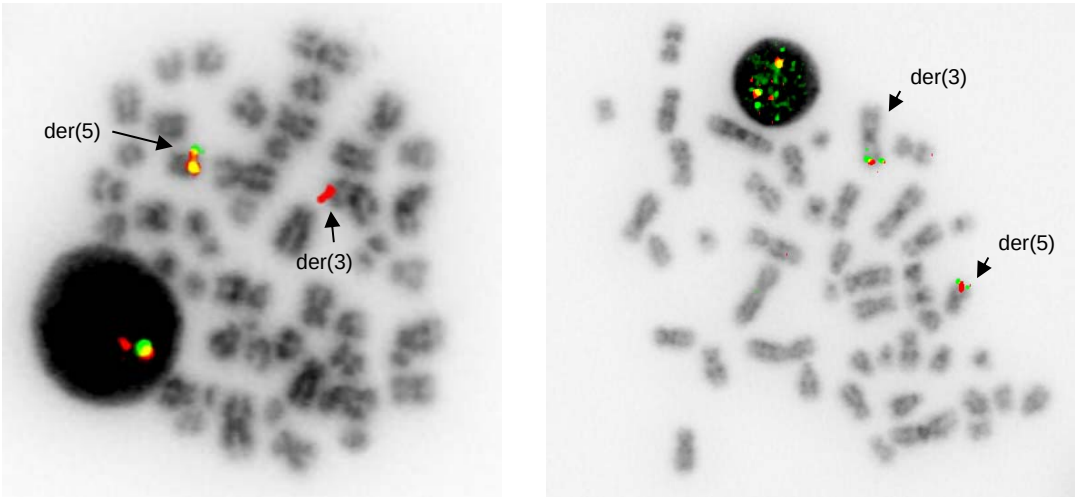
der(5)
der(3)
der(3)
der(5)

C

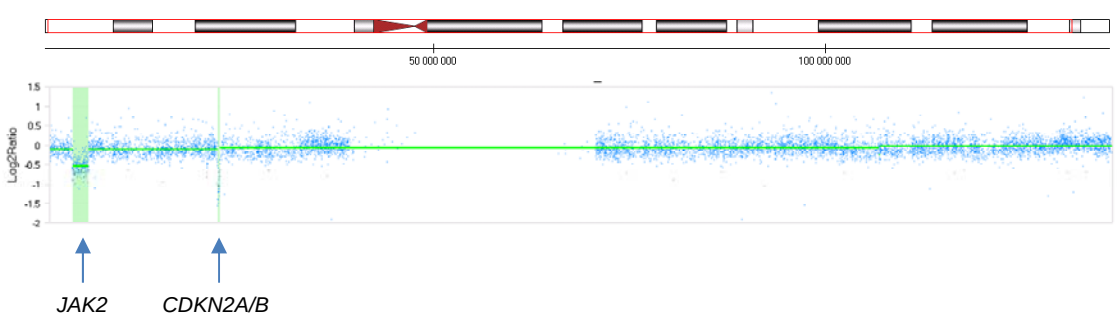
50 000 000
100 000 000
Log2Ratio
JAK2
CDKN2A/B

D

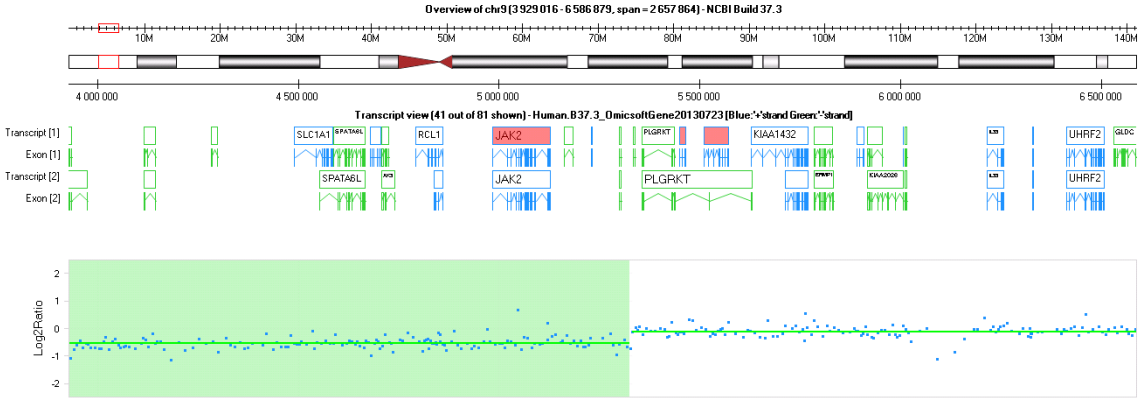
Overview of chr9 (3 929 016 - 6 586 879, span = 2 657 864) - NCBI Build 37.3
Transcript view (41 out of 81 shown) - Human.B37.3_OmicsoftGene20130723 [Blue:'+'strand Green:'-'strand]
Transcript [1]
Exon [1]
Transcript [2]
Exon [2]
SLC1A1
SPATA6L
RCL1
JAK2
PLGRKT
KIAA1432
UHRF2
Log2Ratio

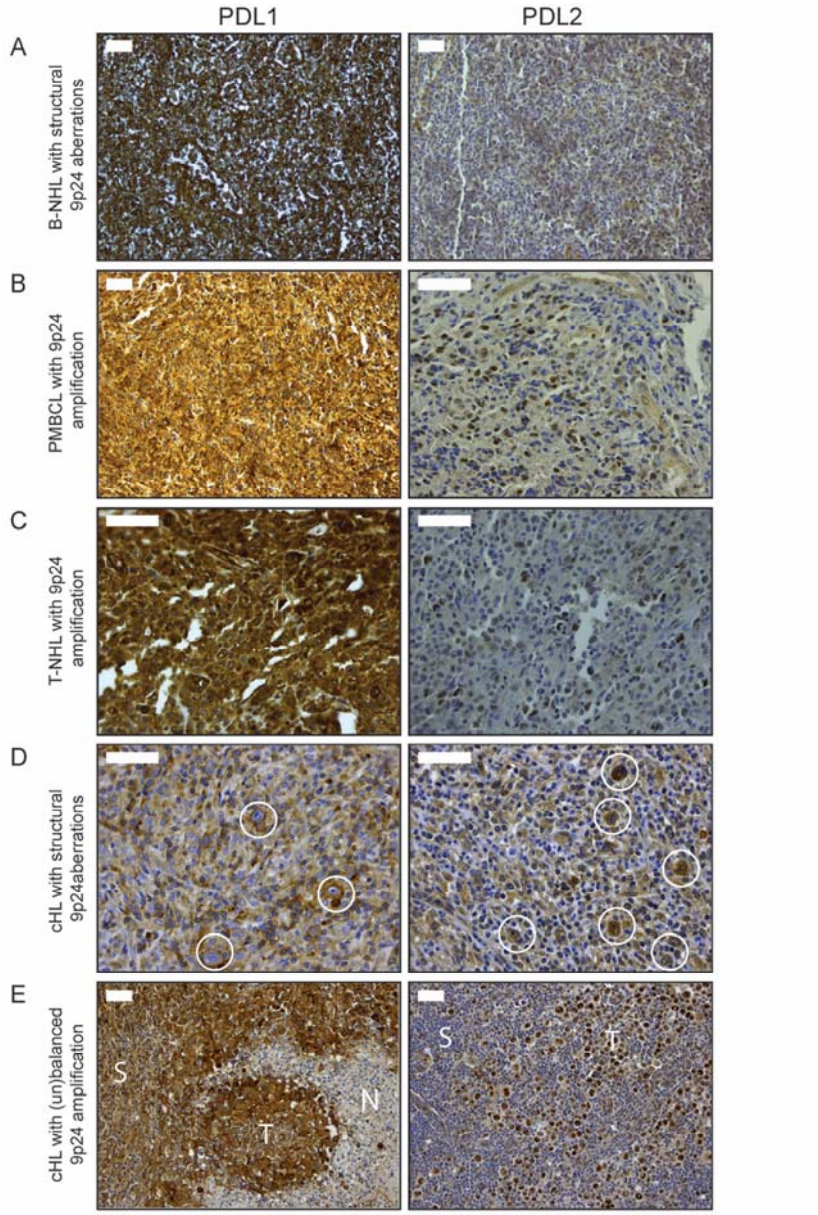
PDL1
PDL2
A
B-NHL with structural 9p24 aberrations
B
PMBCL with 9p24 amplification
C
T-NHL with 9p24 amplification
D
cHL with structural 9p24aberrations
E
cHL with (un)balanced 9p24 amplification
S
T
N
S
T

Figure S2